

# Comparison of biventricular ejection fractions using cadmium-zinc-telluride SPECT and planar equilibrium radionuclide angiography

Yi-Chieh Chen, MSc,<sup>a</sup> Chi-Lun Ko, MD,<sup>b</sup> Rouh-Fang Yen, MD, PhD,<sup>a</sup>  
Mei-Fang Lo, Bsc,<sup>a</sup> Yih-Hwen Huang, MSc,<sup>a,c</sup> Pei-Ying Hsu, MD,<sup>b</sup>  
Yen-Wen Wu, MD, PhD,<sup>a,d,e,f</sup> and Mei-Fang Cheng, MD<sup>a,g</sup>

<sup>a</sup> Department of Nuclear Medicine, National Taiwan University Hospital and National Taiwan University College of Medicine, Taipei, Taiwan

<sup>b</sup> Department of Nuclear Medicine, National Taiwan University Hospital Yun-Lin Branch, Douliou City, Yunlin County, Taiwan

<sup>c</sup> Department of Electrical Engineering, National Taiwan University, Taipei, Taiwan

<sup>d</sup> Department of Nuclear Medicine, Far Eastern Memorial Hospital, New Taipei City, Taiwan

<sup>e</sup> Cardiology Division of Cardiovascular Medical Center, Far Eastern Memorial Hospital, New Taipei City, Taiwan

<sup>f</sup> School of Medicine, National Yang-Ming University, Taipei, Taiwan

<sup>g</sup> Institute of Occupational Medicine and Industrial Hygiene, National Taiwan University, Taipei, Taiwan

Received May 22, 2015; accepted Nov 29, 2015

doi:10.1007/s12350-015-0367-1

**Background.** We compared biventricular ejection fractions (EFs) from gated blood-pool single-photon emission computed tomography (SPECT) using a cadmium-zinc-telluride camera (CZT-SPECT) with planar equilibrium radionuclide angiography (ERNA) using a NaI gamma camera (NaI-planar). We also evaluated whether imaging time can be reduced without compromising image quality using the CZT camera.

**Methods.** Forty-eight patients underwent NaI-planar and CZT-SPECT on the same day. CZT-SPECT datasets were re-projected at an LAO orientation similar to ERNA acquisition, forming CZT-repro planar datasets. The resulting biventricular volumetric measurements and EFs were compared.

**Results.** LVEF calculated from CZT-SPECT and CZT-repro correlated better with NaI-planar ( $r = 0.93$  and  $0.99$ , respectively) than RVEF ( $r = 0.76$  and  $0.82$ , respectively). Excellent intra-class correlation and low bias in intra-observer comparisons were observed for the biventricular EFs derived from three datasets. A wider limit of agreement in CZT-SPECT-derived LVEFs, lower correlation and significant bias for NaI-planar, and CZT-repro-derived RVEFs was found in the inter-observer analyses. Nonetheless, the imaging time can be reduced to 4 minutes without increasing variability in EFs using the CZT camera ( $P = \text{NS}$ ).

**Conclusions.** LVEFs calculated from CZT-SPECT and CZT-repro correlated well with NaI-planar. CZT camera may reduce imaging time while preserving image quality in the assessment of biventricular EFs. (J Nucl Cardiol 2016;23:348–61.)

**Antecedentes.** Se compararon las fracciones de eyección (FsE) bi ventriculares de la ventriculografía SPECT (single photon emission computed tomography, por sus siglas en ingles)

Yen-Wen Wu and Mei-Fang Cheng contributed equally to the study.  
JNC thanks Dr. E. Alexanderson, UNAM, Mexico for providing the Spanish abstract.

Reprint requests: Yen-Wen Wu, MD, PhD, Cardiology Division of Cardiovascular Medical Center, Far Eastern Memorial Hospital, No. 21, Sec. 2, Nanya S. Rd., Banciao Dist., New Taipei City, Taiwan;

wuyw0502@gmail.com; Mei-Fang Cheng, MD, Department of Nuclear Medicine, National Taiwan University Hospital and National Taiwan University College of Medicine, No. 7, Chung-Shan South Road, Taipei, Taiwan; meifang@ntuh.gov.tw  
1071-3581/\$34.00

Copyright © 2016 American Society of Nuclear Cardiology.

utilizando una cámara de Cadmio-Zinc-Teluro (CZT-SPECT) y de la Ventriculografía Radioisotópica Planar en Equilibrio (VRIE) utilizando una gammacámara de NaI (NaI-Planar). También se evaluó si el tiempo de adquisición de las imágenes se puede reducir sin comprometer la calidad de imagen mediante la cámara CZT.

**Métodos.** Cuarenta y ocho pacientes fueron sometidos a un estudio de VRIE NaI-planar y un estudio de CZT-SPECT el mismo día. Los datos del CZT-SPECT fueron re-proyectados en OAI similar a la adquisición de la VRIE, formando conjuntos de datos planares CZT-repro. Las mediciones volumétricas bi-ventriculares resultantes y las fracciones de expulsión (FsE) fueron comparadas.

**Resultados.** La FEVI calculada a partir del CZT-SPECT y CZT-repro correlaciono mejor con la VRIE NaI-planar ( $r = 0,93$  y  $0,99$ , respectivamente) que la FEVD ( $r = 0,76$  y  $0,82$ , respectivamente). Se observó una excelente correlación intra-clase y un bajo sesgo en las comparaciones intra-observador para las FsE bi-ventriculares derivadas de los tres conjuntos de datos. Se encontró un rango mas amplio de concordancia para la FEVI por CZT-SPECT, así como una menor correlación y un sesgo significativo para la FEVD por VRIE NaI-planar y CZT-repro en el análisis inter-observador. No obstante, el tiempo de adquisición de las imágenes se puede reducir a 4 minutos sin aumentar la variabilidad en las FsE utilizando la cámara CZT ( $P = NS$ ).

**Conclusiones.** La FEVI calculada a partir del CZT-SPECT y CZT-repro tienen una buena correlación con las de la VRIE NaI-planar. La cámara CZT puede reducir el tiempo de adquisición de imágenes, preservando la calidad de imagen en la evaluación de las FsE bi-ventriculares. (J Nucl Cardiol 2016;23:348–61.)

**Key Words:** Cadmium-zinc-telluride camera • gated blood-pool SPECT • planar equilibrium radionuclide angiography • ventricular ejection fractions

#### Abbreviations

EF	Ejection fraction
SPECT	Single-photon emission computed tomography
ERNA	Equilibrium radionuclide angiography
CZT	Cadmium-zinc-telluride
GBPS	Gated blood-pool SPECT
LAO	Left anterior oblique
LV	Left ventricular
RV	Right ventricular
EDV	End-diastolic volume
ESV	End-systolic volume

---

**See related editorial, pp. 362–365**

---

## INTRODUCTION

Planar equilibrium radionuclide angiography (ERNA) is a well-established and valuable tool in the assessment of biventricular function. Left ventricular ejection fraction (LVEF) measured by  $^{99m}\text{Tc}$ -labeled multi-gated radionuclide angiography is used clinically in monitoring cardiotoxicity during treatment.<sup>1</sup> However, the issue of overlapping cardiac chambers on 2-

dimensional projection images limits planar ERNA to accurately estimate ventricular function. ECG-gated blood-pool single-photon emission computed tomography (GBPS) has the potential to overcome this difficulty. LVEF computed from GBPS was reproducible and correlated well with planar ERNA methods in a large, multicenter study.<sup>2,3</sup> In addition, EF and volume measurements by GBPS exhibit close agreement with cardiac magnetic resonance imaging (MRI) calculation.<sup>4</sup>

The novel dedicated cardiac camera system equipped with cadmium-zinc-telluride (CZT) pixelated detectors improves count sensitivity and spatial resolution, which may allow GBPS to be more feasible clinically by reducing acquisition time.<sup>5–7</sup> Wells et al<sup>8</sup> first demonstrated that re-projected planar images from CZT single-photon emission computed tomography (SPECT) dataset was an effective way to acquire LV functional measurements. Jensen et al<sup>9,10</sup> indicated that LV function derived from SPECT using CZT detectors was less subjective to intra- and inter-observer variations than obtained from a traditional sodium iodide (NaI) camera. However, comparison of RV function derived from a CZT camera and NaI-planar images has yet to be examined.

The aim of this study was to compare biventricular volumetric measurements and EFs obtained from a dedicated CZT cardiac gamma camera using GBPS (CZT-SPECT), the re-projected planar images from GBPS (CZT-repro), and the planar ERNA from a

traditional NaI gamma camera (NaI-planar). In addition, we also investigated if the image acquisition time can be reduced while preserving image quality in the assessment of biventricular EFs using the CZT camera.

## MATERIALS AND METHODS

### Inclusion Criteria

From June 2013 to July 2014, consecutive patients referred to the Department of Nuclear Medicine at the National Taiwan University Hospital for evaluation of cardiac function were included in the study. A total of 48 patients were analyzed: 29 females and 19 males with a mean age of 53.6 years (range 15 to 76 years). Twenty-two patients were referred for cardiac function to monitor cardiotoxicity during their cancer treatments; none had known cardiovascular disease or diabetes. Twenty-six patients were referred for pre-heart transplantation evaluation, among which 12 had coronary artery disease (CAD), 8 dilated cardiomyopathy (DCM), and 6 valvular heart diseases (VHD). In these heart failure patients due to DCM or VHD, none had diabetes, hypertension, or hyperlipidemia. On the other hand, in the 12 patients with history of CAD, all had hypertension, 4 diabetes mellitus, 6 hyperlipidemia, and 2 were cigarette smokers.

After giving informed consent, all participants underwent planar ERNA with a traditional NaI gamma camera followed by GBPS on a dedicated CZT camera on the same day. The study protocol was approved by the Institutional Review Board of National Taiwan University Hospital.

### Gated Equilibrium Radionuclide Angiography with a NaI Camera

All patients underwent standard ERNA using <sup>99m</sup>Tc-labeled red blood cells according to the recommended protocol outlined by the American Society of Nuclear Cardiology.<sup>11</sup> *In vivo* or

modified *in vivo* red blood cells labeled with 925 MBq of <sup>99m</sup>TcO<sub>4</sub><sup>-</sup> were used. Patients were imaged using a dual-head gamma camera (SMV DSTXL, GE Healthcare) equipped with a low-energy high-resolution collimator. The images were acquired ECG-gated to 24 frames per RR interval at the left anterior oblique (LAO) orientation, which allows the best separation of the LV and RV, and recorded in a 64 × 64 matrix with a timing acceptance window of ±15% and a symmetric 10% energy window centered at 140 keV. Six million counts were acquired in the acceptance window.

### Gated Blood Pool SPECT with a Dedicated CZT Cardiac Camera

Immediately after obtaining the planar views, a gated tomographic acquisition was performed using a dedicated cardiac camera (DiscoveryNM530c, GE Healthcare Israel, Tirat Hacarmel, Israel). Projection data were acquired according to previous study<sup>8</sup> for 8 minutes with a 10% energy window centered at 140 keV, and were ECG-gated to 24 frames with an acceptance window of ±15%. The mean total acquired counts were 12.5 ± 5.0 million counts. The projection data were then reconstructed into 24-frame GBPS images (CZT-SPECT) by a maximum likelihood expectation maximization (MLEM)-based algorithm with 30 iterations without attenuation or scatter correction. The voxel size was 4 × 4 × 4 mm<sup>3</sup>.

The CZT-SPECT images were re-projected into 60 parallel forward projections in order to select an LAO orientation, the best septal separation angle, determined from the planar ERNA using the traditional NaI camera. A 24-frame gated planar dataset (CZT-repro) was produced, and subsequently analyzed in the same manner as in NaI-planar dataset.

### Assessments of Biventricular Ejection Fractions and Volumes

In the first 5 studies, two experienced technologists (*Chen YC* and *Lo MF*) and an experienced nuclear medicine physician

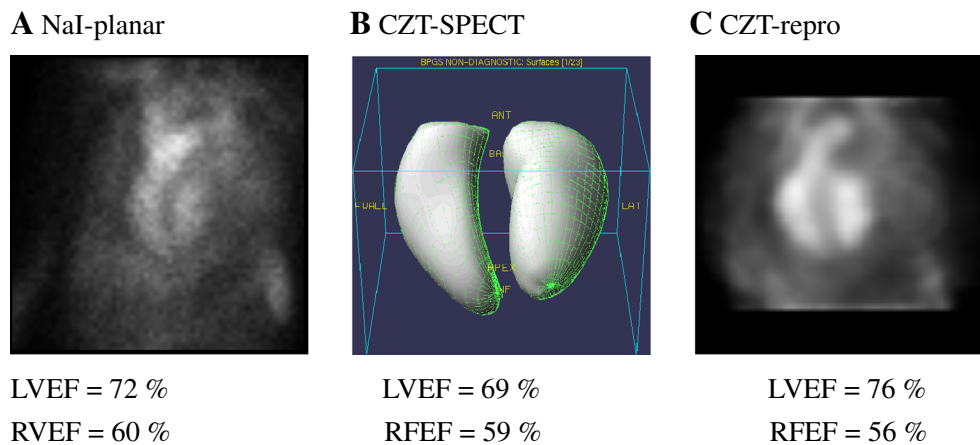


**Figure 1.** Example datasets and calculated ejection fractions from a traditional gamma camera (A), SPECT imaging using a CZT camera (B), and the re-projected planar images from the CZT-SPECT (C) of the same patient.

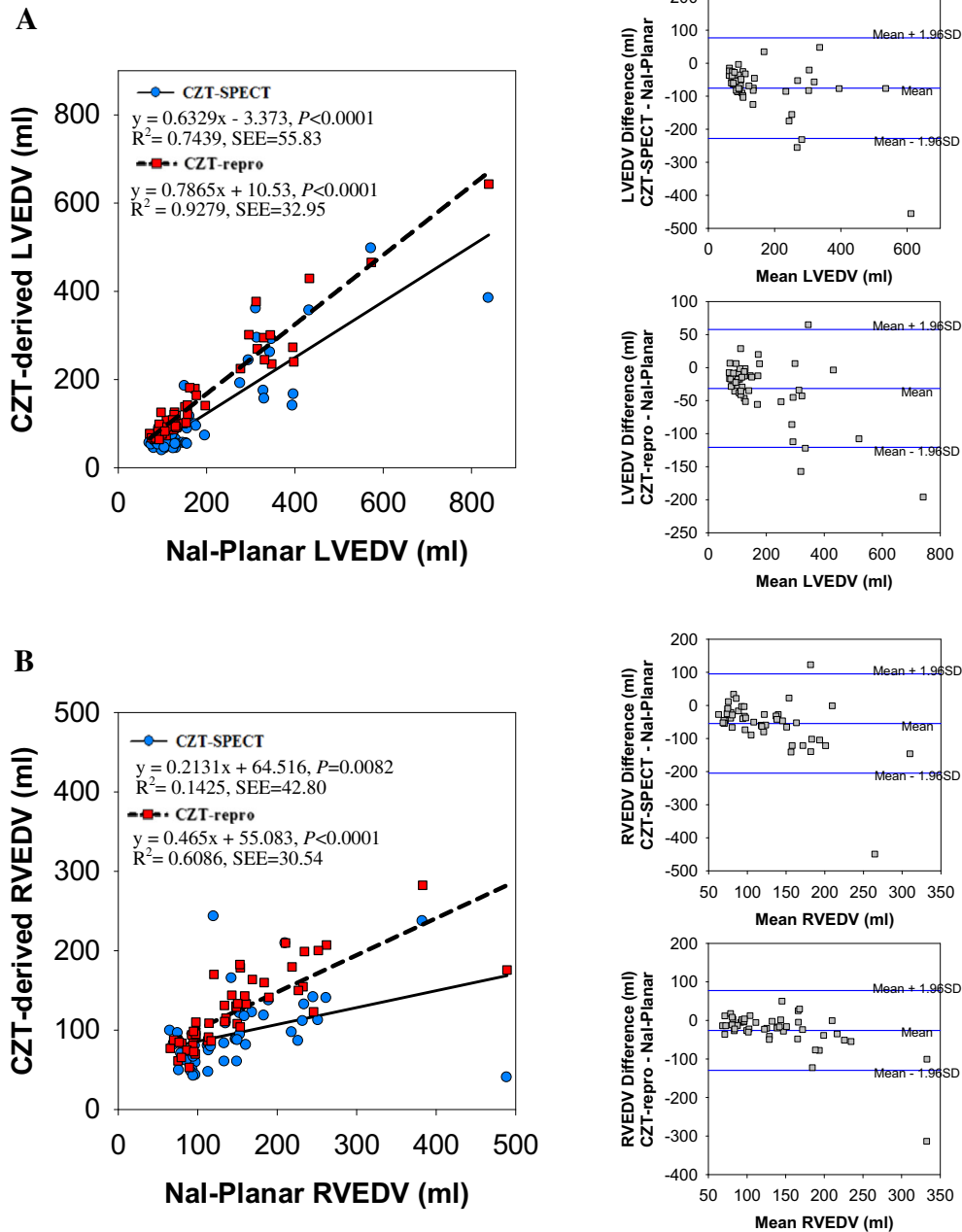


**Figure 2.** Correlation and Bland-Altman plots between NaI-planar and CZT-derived LVEDV (A) and RVEDV (B).

(Chen MF) adjusted the regions of interest (ROIs) and processed together. Then the two technologists who were blinded to patients' clinical data, including EF values from other techniques, processed each acquisition dataset independently in order to avoid any possible bias in the analysis, and the inter-observer variation was analyzed. For the intra-observer analysis, the technologists repeated the analysis for each dataset following an interval of 2 months of the first analysis.

Both the 24-frame gated NaI-planar and CZT-repro images were analyzed at a Vision POWER station (GE healthcare). The LV is detected automatically within a user-

defined region, but can be manually adjusted as needed. The LVEF and RVEF were calculated by drawing ROIs enclosing the left and right ventricles at end-systole (ES) and end-diastole (ED) and counting the difference between the counts at ES and ED divided by the background-corrected counts at ED. The ROI used for background correction was placed 5 to 10 mm away from the end-diastolic border, avoiding any activity from the aorta or spleen.<sup>11</sup> Ventricular volumes were calculated using the count-based method: the ratio of the maximum counts in the ROI to the total counts in a pixel.<sup>12</sup>

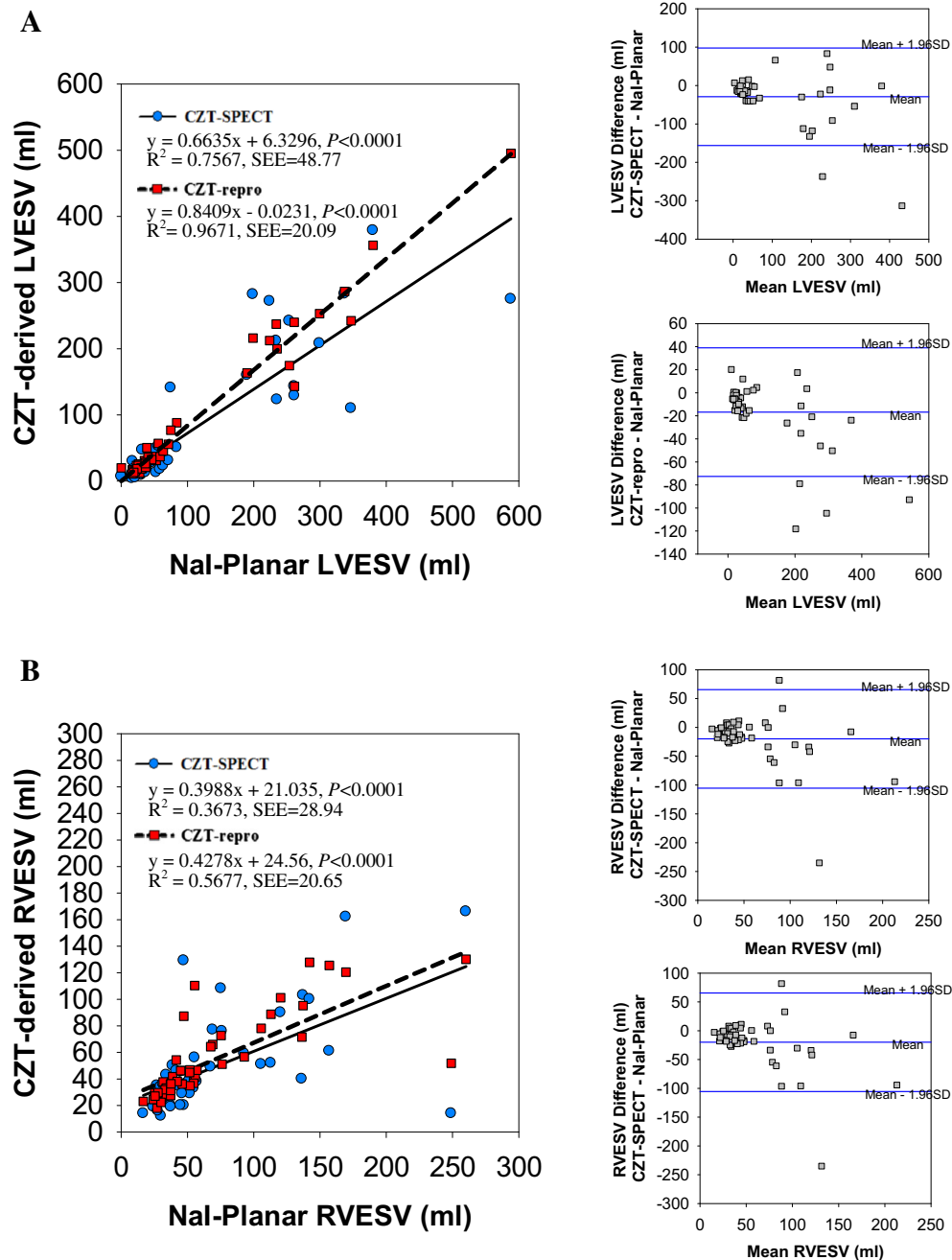


**Figure 3.** Correlation and Bland-Altman plots between NaI-planar and CZT-derived LVESV (A) and RVESV (B).

The matrix size of CZT-SPECT images was extracted from  $70 \times 70$  to  $64 \times 64$ , and analyzed using Quantitative Blood-Pool SPECT (QBS; Cedars Sinai, USA) software that automatically calculates the LVEF and RVEF.<sup>13</sup> After the transaxial slices were reoriented into the usual cardiac axis, the QBS algorithm was then applied to the data for ventricular segmentation for each interval. The generation of endocardial surfaces was processed using a variable-threshold method based on dynamic computation from data gradient information. These endocardial surfaces were then

used to compute ventricular volumes at each interval allowing the calculation of ED and ES intervals. The biventricular EFs were calculated using these intervals.

### Reduction of Imaging Acquisition Time

The CZT-SPECT dataset was acquired in the list-mode for 8 minutes,<sup>8</sup> and processed by a built-in software (Lister, GE Healthcare). The dataset was clipped into 16-frame gated

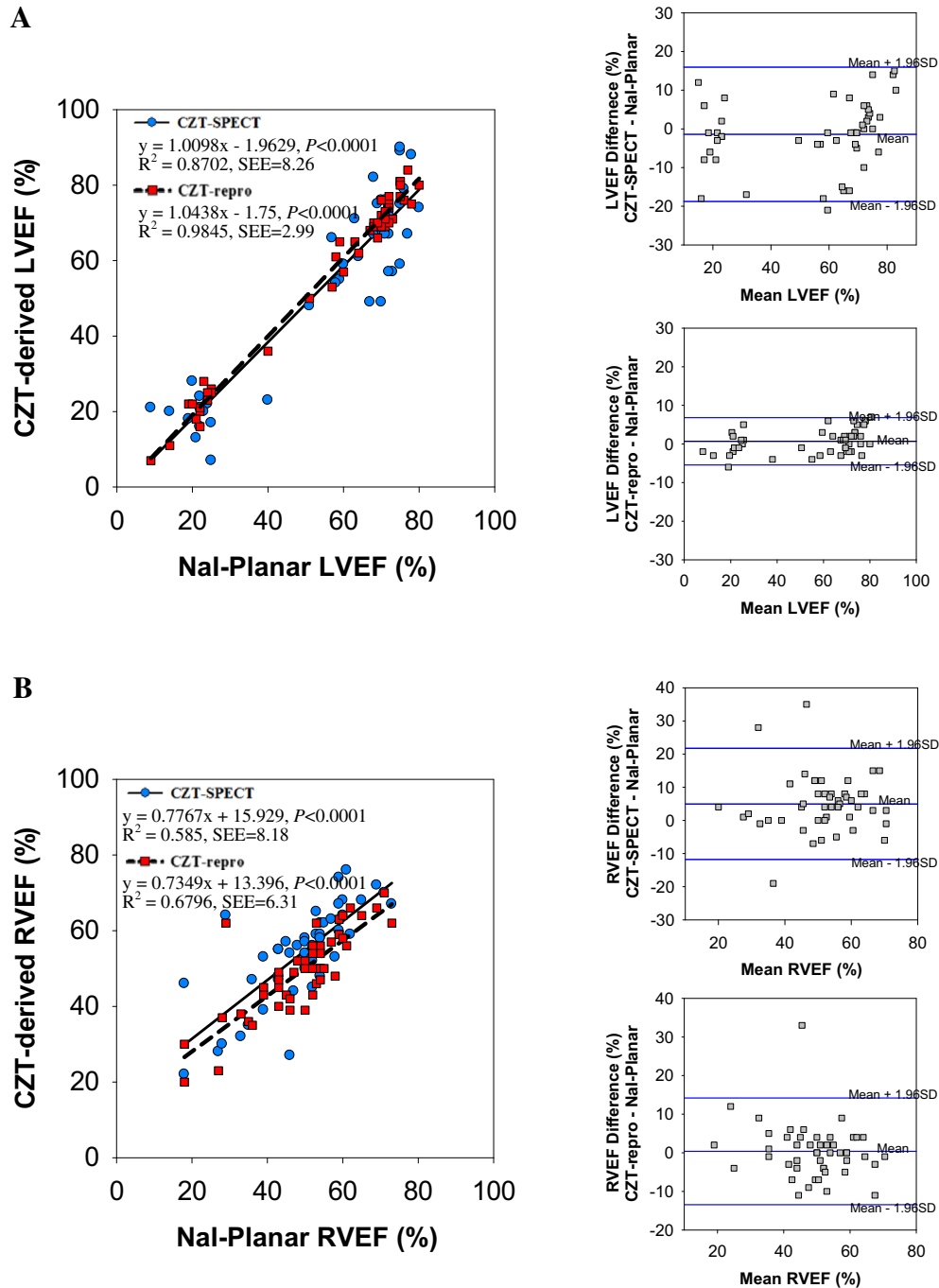


**Figure 4.** Correlation and Bland-Altman plots between Nal-planar and CZT-derived LVEF (A) and RVEF (B).

projections of 1, 2, 3, 4, 5, 6, and 8 minutes, and then reconstructed into SPECT images. Biventricular EFs were determined using Quantitative Blood-Pool SPECT software for all images by the same technologist. To determine if image acquisition time can be reduced using CZT-SPECT for EF measurements, a standard variation derived from an intra-observer study using the standard 8-minute protocol was used

for comparison. The reprocessed 8-minute CZT-SPECT images were analyzed twice within 3 months by the same technologist.

### Statistical Analysis

All measured values were presented as mean  $\pm$  standard deviation (SD). An un-blinded comparison of parametric data

between the three datasets was made by using one-way ANOVA with post hoc Tukey's test. Comparisons between continuous and categorical variables were performed using Student's *t* test and  $\chi^2$  analysis, respectively. Correlation between continuous variables was assessed by Pearson's correlation tests as follows:  $r = 0$ , poor; 0.01-0.20, slight; 0.21-0.40, fair; 0.41-0.60, moderate; 0.61-0.80, good; 0.81-1.00, excellent. Agreement between measurements was assessed by the Bland-Altman method.

To assess the inter- and intra-observer variability, the bias estimated by the mean difference, SD of the difference, and 95% confidence interval (CI) of the difference was calculated from Bland-Altman method. *F* test was applied to compare the variances of 2 samples. Each statistical test was 2-sided, and a *P* value of  $< .05$  was considered statistically significant. All data were analyzed using SigmaPlot 12.0 (SystatSoftware Inc.).

## RESULTS

Biventricular ejection fractions and volumetric measurements were determined for each patient using the three imaging techniques. Examples of EFs calculated using NaI-planar, CZT-SPECT, and CZT-repro are shown in Figure 1.

### LVEF and Volumes

The mean values of LVEDV for NaI-planar, CZT-SPECT, and CZT-repro were  $197.2 \pm 148.7$ ,  $121.4 \pm 109.2$ , and  $165.6 \pm 121.4$  ml, respectively. For the LVESV, the corresponding values were  $105.5 \pm 128.2$ ,  $76.3 \pm 97.8$ , and  $88.7 \pm 109.6$  ml. LVEDV values were significantly higher for the NaI-planar compared to both the CZT-SPECT and CZT-repro methods (all  $P < .05$ ). There was no significant difference in mean LVESV among three datasets. There were excellent correlations of LVEDV and LVESV between NaI-planar and CZT-derived datasets (NaI-planar vs. CZT-SPECT:  $r = 0.86$  and  $0.87$  for LVEDV and LVESV, respectively; NaI-planar vs. CZT-repro:  $r = 0.96$  and  $0.98$ , respectively; all  $P < .001$ ) (Figures 2A, 3A). Compared with NaI-planar, CZT-derived LVEDV and LVESV were underestimated as LV enlarged ( $P < .001$ ).

There was no significant difference in mean LVEFs derived from NaI-planar, CZT-SPECT, and CZT-repro ( $55.7 \pm 22.7$ ,  $54.3 \pm 24.6$ , and  $56.4 \pm 23.9\%$ , respectively;  $P = \text{NS}$ ). Comparison of LVEFs from NaI-planar and CZT-derived datasets yielded excellent correlations (NaI-planar vs. CZT-SPECT:  $r = 0.93$ ; NaI-planar vs. CZT-repro:  $r = 0.99$ ; both  $P < .001$ ) (Figure 4A). Bland-Altman analysis showed no statistically significant trend for the bias of LVEF from the CZT-SPECT and CZT-repro compared with NaI-planar (Figure 4A).

We divided the patients into two subgroups according to NaI-planar-derived LVEFs (group1: LVEF  $\geq 35\%$ ; group2: LVEF  $< 35\%$ ). For both groups, no significant

differences in LVEFs derived from NaI-planar, CZT-SPECT and CZT-repro were observed (group 1:  $68.6 \pm 8.1$ ,  $67.3 \pm 13.3$ , and  $69.7 \pm 9.6\%$ , respectively;  $n = 35$ ,  $P = \text{NS}$ ; group 2:  $20.8 \pm 4.6$ ,  $19.2 \pm 5.2$ , and  $20.3 \pm 6.0\%$ , respectively;  $n = 13$ ,  $P = \text{NS}$ ). The relationships between NaI-planar and CZT-derived LVEFs for these two subgroups were presented in Figure 5. Correlations between NaI-planar and both CZT-derived two datasets were significantly better in patients with LVEF  $\geq 35\%$  (group 1) than those with LVEF  $< 35\%$  (group 2). Moreover, LVEFs derived from NaI-planar and CZT-SPECT showed rather poor correlation in patients with LVEF  $< 35\%$ .

### RVEF and Volumes

The mean values of RVEDV for NaI-planar, CZT-SPECT, and CZT-repro were  $151.6 \pm 81.0$ ,  $96.8 \pm 45.7$ , and  $125.6 \pm 48.3$  ml, respectively. For the RVESV, the corresponding values were  $68.1 \pm 54.7$ ,  $48.2 \pm 36.0$ , and  $53.7 \pm 31.1$  ml. RVEDV values were significantly higher

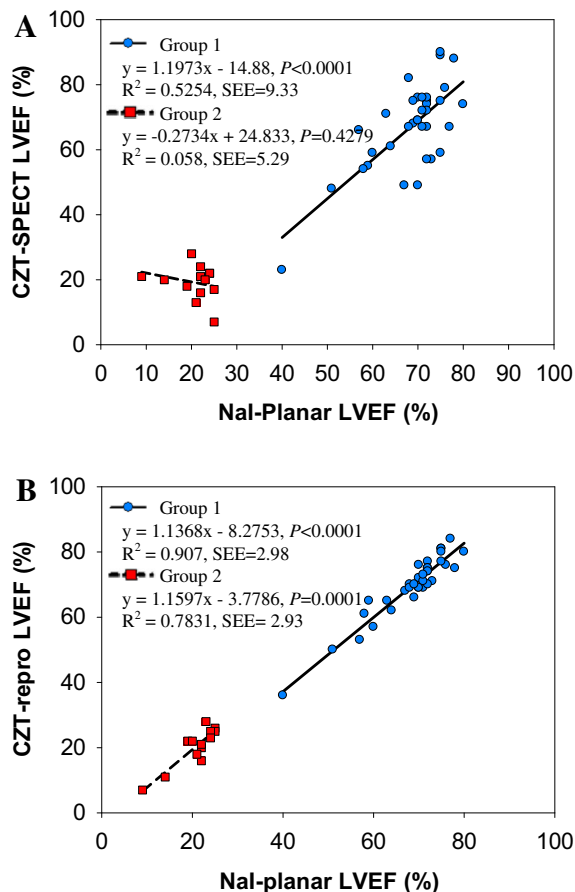


**Figure 5.** Correlation plots between LVEFs derived from NaI and CZT cameras (Group 1: LVEF  $\geq 35\%$ ; Group 2: LVEF  $< 35\%$ ).

**Table 1.** Inter-observer agreement by Bland-Altman method

	<b>LVEF% (95% CI)</b>	<b>LVEDV% (95% CI)</b>	<b>LVESV% (95% CI)</b>	<b>RVEF% (95% CI)</b>	<b>RVEDV% (95% CI)</b>	<b>RVESV% (95% CI)</b>
Nal-planar						
ICC	0.96	0.95	0.97	0.70	0.91	0.89
Mean Difference	-0.44 (-2.09 to 1.21) <sup>c</sup>	39.53 (30.64 to 48.42) <sup>a</sup>	6.78 (-2.52 to 16.08) <sup>c</sup>	-4.08 (-6.36 to -1.81) <sup>a</sup>	22.54 (14.18 to 30.89) <sup>a</sup>	15.85 (9.09 to 22.61) <sup>a</sup>
Upper LOA	10.72 (7.86 to 13.57)	99.60 (84.20 to 114.99)	69.63 (53.52 to 85.73)	11.3 (7.36 to 15.24)	79.01 (64.54 to 93.48)	61.55 (49.84 to 73.26)
Lower LOA	-11.59 (-14.45 to -8.73)	-20.53 (-35.93 to -5.14)	-56.07 (-72.17 to -39.97)	-19.47 (-23.41 to -15.53)	-33.94 (-48.41 to -19.47)	-29.86 (-41.57 to -18.14)
Std	3.99	15.95	22.94	6.2	25.7	19.79
CZT-SPECT						
ICC	0.92	0.87	0.89	0.85	0.87	0.92
Mean Difference	-0.1 (-2.96 to 2.75) <sup>c</sup>	9.81 (-7.15 to 26.78) <sup>c</sup>	8.67 (-5.30 to 22.64) <sup>c</sup>	-0.1 (-2.29 to 2.08) <sup>c</sup>	-4.54 (-11.87 to 2.79) <sup>c</sup>	-1.73 (-6.14 to 2.68) <sup>c</sup>
Upper LOA	19.19 (14.25 to 24.14)	124.48 (95.10 to 153.87)	103.10 (78.90 to 127.30)	14.68 (10.89 to 18.47)	45.01 (32.31 to 57.71)	28.09 (20.45 to 35.73)
Lower LOA	-19.4 (-24.35 to -14.46)	-104.86 (-134.24 to -75.47)	-85.77 (-109.97 to -61.57)	-14.89 (-18.68 to -11.10)	-54.09 (-66.79 to -41.40)	-31.54 (-39.18 to -23.90)
Std	6.89 <sup>d</sup>	34.60 <sup>d</sup>	34.26 <sup>e</sup>	5.28 <sup>f</sup>	17.98 <sup>f</sup>	10.71 <sup>e</sup>
CZT-repro						
ICC	0.95	0.94	0.96	0.54	0.83	0.63
Mean Difference	-2.88 (-4.80 to -0.95) <sup>b</sup>	35.83 (25.20 to 46.46) <sup>a</sup>	16.22 (7.25 to 25.18) <sup>a</sup>	-6.27 (-8.59 to -3.95) <sup>a</sup>	-3.88 (-14.11 to 6.35) <sup>c</sup>	9.95 (0.98 to 18.91) <sup>b</sup>
Upper LOA	10.13 (6.80 to 13.46)	107.67 (89.26 to 126.08)	76.81 (61.28 to 92.34)	9.42 (5.40 to 13.44)	65.27 (47.55 to 82.98)	70.57 (55.03 to 86.10)
Lower LOA	-15.88 (-19.21 to -12.55)	-36.01 (-54.42 to -17.60)	-44.38 (-59.91 to -28.85)	-21.96 (-25.98 to -17.94)	-73.02 (-90.74 to -55.31)	-50.68 (-66.21 to -35.14)
Std	5.07 <sup>f</sup>	17.99 <sup>f</sup>	24.48 <sup>f</sup>	7.14 <sup>f</sup>	24.84 <sup>f</sup>	22.76 <sup>f</sup>

CI, Confidence interval; ICC, intra-class correlation; LOA, limit of agreement; NS, not significant  
<sup>a</sup>*P* < 0.001; <sup>b</sup>*P* < 0.05; <sup>c</sup>*P* = NS; using *T* test  
<sup>d</sup>*P* < 0.001; <sup>e</sup>*P* < 0.05; <sup>f</sup>*P* = NS, using *F* test to compare the variances with Nal-planar



**Table 2.** Intra-observer agreement by Bland-Altman method

	<b>LVEF%</b> <b>(95% CI)</b>	<b>LVEDV%</b> <b>(95% CI)</b>	<b>LVESV%</b> <b>(95% CI)</b>	<b>RVEF%</b> <b>(95% CI)</b>	<b>RVEDV%</b> <b>(95% CI)</b>	<b>RVESV%</b> <b>(95% CI)</b>
Nal-planar						
ICC	0.99	0.98	0.98	0.92	0.95	0.93
Mean Difference	-0.65 (-1.75 to 0.46) <sup>c</sup>	4.31 (-3.81 to 12.43) <sup>c</sup>	6.37 (-1.64 to 14.38) <sup>c</sup>	-0.65 (-2.12 to 0.82) <sup>c</sup>	2.29 (-5.25 to 9.84) <sup>c</sup>	4.51 (-1.83 to 10.86) <sup>c</sup>
Upper LOA	6.85 (4.93 to 8.77)	59.17 (45.11 to 73.23)	60.50 (46.63 to 74.37)	9.29 (6.74 to 11.83)	53.30 (40.23 to 66.36)	47.42 (36.42 to 58.41)
Lower LOA	-8.14 (-10.06 to -6.21)	-50.56 (-64.62 to -36.50)	-47.76 (-61.63 to -33.89)	-10.58 (-13.12 to -8.03)	-48.71 (-61.78 to -35.64)	-38.39 (-49.38 to -27.40)
Std	2.71	19.82	19.84	3.58	18.28	15.65
CZT-SPECT						
ICC	0.98	0.97	0.98	0.94	0.95	0.98
Mean Difference	-1.02 (-2.41 to 0.37) <sup>c</sup>	-8.46 (-15.65 to -1.26) <sup>b</sup>	-5.69 (-11.58 to 0.21) <sup>c</sup>	-1.13 (-2.36 to 0.11) <sup>c</sup>	-6.48 (-10.32 to -2.64) <sup>b</sup>	-2.81 (-4.93 to -0.69) <sup>b</sup>
Upper LOA	8.39 (5.98 to 10.80)	40.18 (27.72 to 52.65)	34.16 (23.95 to 44.37)	7.22 (5.08 to 9.35)	19.46 (12.81 to 26.11)	11.50 (7.83 to 15.17)
Lower LOA	-10.43 (-12.84 to -8.02)	-57.10 (-69.56 to -44.63)	-45.54 (-55.75 to -35.32)	-9.47 (-11.60 to -7.33)	-32.42 (-39.07 to -25.77)	-17.13 (-20.80 to -13.46)
Std	3.44 <sup>f</sup>	18.36 <sup>f</sup>	14.78 <sup>e</sup>	3.08 <sup>f</sup>	10.33 <sup>d</sup>	5.48 <sup>d</sup>
CZT-repro						
ICC	0.99	0.92	0.95	0.87	0.81	0.89
Mean Difference	0.81 (-0.18 to 1.80) <sup>c</sup>	16.92 (2.94 to 30.90) <sup>b</sup>	7.12 (-2.85 to 17.09) <sup>c</sup>	1.29 (-0.26 to 2.84) <sup>c</sup>	17.47 (8.53 to 26.40) <sup>a</sup>	4.35 (-0.24 to 8.94) <sup>c</sup>
Upper LOA	7.49 (5.78 to 9.20)	111.43 (87.21 to 135.64)	74.49 (57.22 to 91.75)	11.78 (9.09 to 14.47)	77.86 (62.39 to 93.34)	35.38 (27.43 to 43.34)
Lower LOA	-5.86 (-7.57 to -4.15)	-77.58 (-101.80 to -53.36)	-60.25 (-77.51 to -42.99)	-9.20 (-11.88 to -6.51)	-42.93 (-58.40 to -27.45)	-26.68 (-34.64 to -18.73)
Std	2.45 <sup>f</sup>	35.80 <sup>d</sup>	24.57 <sup>f</sup>	3.85 <sup>f</sup>	24.85 <sup>f</sup>	11.50 <sup>e</sup>

CI, Confidence interval; ICC, intra-class correlation; LOA, limit of agreement; NS, not significant  
<sup>a</sup> $P < 0.001$ , <sup>b</sup> $P < 0.05$ , <sup>c</sup> $P = NS$ , using  $T$  test  
<sup>d</sup> $P < 0.001$ , <sup>e</sup> $P < 0.05$ , <sup>f</sup> $P = NS$ , using  $F$  test to compare the variances with Nal-planar

for the NaI-planar compared to both the CZT-SPECT and CZT-repro methods (both  $P < .001$ ). There was only marginal difference in mean RVESV among the three datasets ( $P = .062$ ). RVEDV and RVESV from NaI-planar and CZT-repro showed good correlation (RVEDV,  $r = 0.78$ ; RVESV,  $r = 0.75$ ; both  $P < .001$ ). Slightly less but fair correlation was noted between NaI-planar and CZT-SPECT (RVEDV,  $r = 0.39$ ; RVESV,  $r = 0.61$ ; both  $P < .05$ ). As in LV volumes, CZT-derived RVEDV and RVESV were also underestimated as RV enlarges ( $P < .001$ ) (Figures 2B, 3B).

There was only borderline difference in mean RVEFs derived from NaI-planar, CZT-SPECT, and CZT-repro ( $49.1 \pm 12.4$ ,  $54.1 \pm 12.6$ , and  $49.5 \pm 11.0\%$ , respectively;  $P = .078$ ). Comparisons of RVEFs yielded excellent correlation between NaI-planar and CZT-repro ( $r = 0.82$ ,  $P < .001$ ), and good correlation between NaI-planar and CZT-SPECT ( $r = 0.76$ ,  $P < .001$ ). Bland-Altman analysis showed no statistically significant trend ( $P = NS$ ) of bias between NaI-planar and CZT-derived RVEF (Figure 4B).

### Reproducibility

Intra- and inter-observer variability on biventricular EFs and volumes are presented in Tables 1 and 2, respectively. The intra-observer study revealed excellent intra-class correlation ( $P < .001$ ) for all measurements of biventricular functions in three datasets. No significant intra-observer bias was found in all measurements from NaI-planar ( $P = NS$ ). For the CZT-SPECT, significant bias were found in the measurements of LVEDV, RVEDV, and RVESV (all  $P < .05$ ). For the CZT-repro, significant bias were also found in the measurements of LVEDV and RVEDV ( $P < .05$ ). *F* test showed the intra-observer variances were lower for LVESV, RVEDV, and RVESV calculated from CZT-SPECT than NaI-planar and lower for RVESV (both

$P < .05$ ), but higher for LVEDV ( $P < .001$ ) from CZT-repro than NaI-planar methods.

The inter-observer study revealed excellent intra-class correlation ( $P < .001$ ) for all measurements of biventricular functions in three datasets except for RVEF derived from NaI-planar and CZT-repro ( $r = 0.70$  and  $0.54$ , respectively) and RVESV derived from CZT-repro ( $r = 0.63$ ). The inter-observer study showed no significant bias in all measurements calculated from CZT-SPECT ( $P = NS$ ). However, significant inter-observer biases were found in the measurements derived from NaI-planar and CZT-repro datasets (Table 1). *F* test showed the inter-observer variances were higher for LVEF, LVEDV, and LVESV but lower for RVESV in CZT-SPECT than in NaI-planar ( $P < .05$ ), while there was no significant difference between NaI-planar and CZT-repro for all measurements ( $P = NS$ ).

### Reduction of Imaging Acquisition Time

EFs were measured from an 8-minute acquisition time as in a previous published study.<sup>8</sup> The acquired total counts for reprocessed images from 1 to 8 minutes were proportional to the image acquisition times (Table 3).

Bland-Altman-derived limits of agreement for the reduced imaging time are presented in Table 4. There was no significant bias in LVEFs for all reduced imaging time from 1 to 6 minutes compared to that of 8 minutes ( $P = NS$ ). However, there was a significant positive bias in RVEF values for 1-, 2-, and 3-minute images compared to that of the 8-minute image ( $P = .002$ ,  $.002$ , and  $.004$ , respectively; Table 3).

In order to evaluate whether the derived EF values from the reduced imaging time were comparable, an intra-observer study was repeated within 3 months using the 8-minute CZT-SPECT datasets. The mean difference

**Table 3.** The total counts and mean values of ejection fraction (%) at various acquisition time using CZT-SPECT

Time (min)	LVEF ± SD (%)	<i>P</i> value*	RVEF ± SD (%)	<i>P</i> value*	<i>M</i> <sub>counts</sub> ± SD
1	54.5 ± 26.4	0.167	53.1 ± 16.3	0.002	1.6 ± 0.6
2	51.4 ± 26.9	0.600	51.5 ± 15.3	0.002	3.2 ± 1.3
3	51 ± 27.2	0.573	49.8 ± 13.5	0.004	4.8 ± 1.9
4	49.8 ± 25.4	0.492	48.6 ± 13.7	0.054	6.3 ± 2.5
5	50.3 ± 26.4	0.801	47.4 ± 14.4	0.359	7.9 ± 3.1
6	50.6 ± 25.4	0.853	48.4 ± 14.3	0.150	9.4 ± 3.7
8	50.5 ± 24.8		46.6 ± 13.4		12.5 ± 5.0

\* *P* value comparing reduced imaging time with 8 minutes  
LVEF, left ventricular ejection fraction; RVEF, right ventricular ejection fraction; *M*<sub>counts</sub>, 10<sup>6</sup> counts

for intra-observer agreement (95% limits of agreement) was  $-1.59\%$  ( $-9.46$  to  $6.28$ ) and  $1.78\%$  ( $-6.78$  to  $10.34$ ) for LVEF and RVEF, respectively. There was no significant difference in the variance between acquisition duration above 3 minutes compared with the 8 minutes for both LVEF and RVEF (all  $F$  test,  $P = NS$ ).

## DISCUSSION

This study demonstrated CZT-repro correlated well with NaI-planar in the measurements of biventricular EF, EDV, and ESV. These results were comparable to previous studies which showed LVEF obtained from the re-projection of the dedicated cardiac SPECT correlated well with the traditional planar images.<sup>8,14</sup> Our study validates previous suggestions that the re-projected planar method using a dedicated cardiac CZT camera can be used as a substitute for planar ERNA. The main advantage of the re-projected planar image is its ability to reorient the tomograms after data acquisition, hence optimizing the separation of the two ventricles. This process reduces the time needed to sequentially reposition the detectors in search of the best septal view, a situation that can be difficult in cases with low count rates.

Previous studies have demonstrated that GBPS is highly reproducible and correlated well with planar RNA and cardiac MRI for EFs and volume measurements.<sup>3,4,15</sup> In the subgroup analysis, patients with LVEF  $< 35\%$  calculated from NaI-planar showed no significant correlation with CZT-SPECT. One possible explanation is incorrect septal separation or overlap in enlarged LV or RV by planar image; or this could be due to incorrect identification of endocardium by the automatic QBS software in these patients, that were often presented with dilated and dysfunctional LV. The attenuation defects in the center of the LV were noted in patients with severely dilated LV; and the relative effect of photon attenuation at ED and ES may have some impact on the calculated LVEF.<sup>3</sup> Regrettably, the measured LVEFs from different modalities in the current study were not compared with cardiac MRI, which is the major limitation of our study.

Slightly lower correlation for RVEFs was also reported in several studies.<sup>15,16</sup> Similarly, better correlation coefficients between NaI-planar and CZT-SPECT with regard to LV than in RV parameters were also observed in our study. Although tomographic RNA provides better separation of the right ventricle from the right atrium,<sup>17</sup> the detection of RV boarder using QBS software is influenced by the size and shape of the LV. The detection algorithm may not be accurate when the RV chamber is dilated, resulting in decreased correlation with planar RNA. The average RVEF from CZT-SPECT

was 5% higher than that from NaI-planar in our study, probably due to better isolation of the RV from RA activity. This is consistent with previous NaI SPECT study which reported 7% higher than in planar images.<sup>16,18</sup>

ERNA has been the preferred method for monitoring LV function in patients receiving cardiotoxic chemotherapy. Since a decline of 10% or more in LVEF is the criteria for predicting heart failure as a complication of chemotherapy,<sup>19</sup> variation in LVEF measurements is of concern. Our results showed excellent intra-class correlation and low bias (mean difference close to zero) with regard to inter- and intra-observer study in three modalities when assessing LVEF, but a slightly wider limit of agreement in the CZT-SPECT between two observers. Regarding the RVEF, the inter-observer study showed lower intra-class correlation and significant mean difference in the two planar image modalities. This difference in estimating the RVEF by planar RNA images may be associated with the right atrium overlapping, which influenced RV region determination. It suggested the importance of training and standardization of adjustment of septal view and the ROIs placement for RV in NaI-planar and CZT-repro methods.

Finally, the effective radiation dose and the acquisition time can be considerably decreased while preserving a high image quality using the CZT camera.<sup>20,21</sup> Our study showed that the acquired total counts were in proportion to the reprocessed acquisition time. CZT-SPECT-derived LVEF values showed close agreement with 8-minute images, even if the imaging time was reduced to 1 minute, but there was significant bias in RVEF values when the acquisition time was shorter than 4 minutes (Figure 6). These differences are probably due to the processing software used which automatically detects the boundaries of the RV. The ROI for the RV is more difficult to identify due to interference from the RA and pulmonary trunk. However, the variation between intra-observer results and imaging time above 4 minutes compared with that of 8 minutes showed no statistical difference. The results suggest that imaging acquisition time can be reduced to as short as 4 minutes without increasing variability in EF values using the CZT camera. However, this finding needs to be further validated in studies of larger sample size.

Attenuation correction (AC) was not applied in this study since the CZT camera was not equipped with CT. Previous study revealed higher volumes and lower EFs after CT-based AC compared to non-corrected.<sup>22</sup> Attenuation influence with the CZT camera is not known, and needs to be further investigated.<sup>23</sup> A newly developed method can provide a patient-specific nonuniform attenuation coefficient map using only the photopeak

**Table 4.** Bland-Altman analyses comparing the agreement between reduced imaging time and 8-minute acquisition time with CZT-SPECT

	<b>LVEF</b>	<b>6 min</b>	<b>5 min</b>	<b>4 min</b>	<b>3 min</b>	<b>2 min</b>	<b>1 min</b>
Mean Difference (95% CI)	0.09 (−0.93 to 1.12)	−0.22 (−1.98 to 1.54)	−0.69 (−2.71 to 1.33)	0.53 (−1.37 to 2.44)	0.94 (−2.68 to 4.55)	4.03 (−1.79 to 9.85)	
Upper LOA	5.67 (3.89 to 7.45)	9.33 (6.28 to 12.37)	10.27 (6.77 to 13.77)	10.88 (7.58 to 14.18)	20.58 (14.31 to 26.84)	35.63 (25.55 to 45.70)	
Lower LOA	−5.48 (−7.26 to −3.70)	−9.77 (−12.81 to −6.72)	−11.64 (−15.14 to −8.15)	−9.82 (−13.12 to −6.52)	−18.70 (−24.96 to −12.44)	−27.56 (−37.64 to −17.48)	
SD	3.70	4.87	5.59	5.28	10.02	16.12	
P* (F test)	0.059	0.287	0.070	0.133	<0.00001	<0.0000001	
	<b>RVEF</b>	<b>6 min</b>	<b>5 min</b>	<b>4 min</b>	<b>3 min</b>	<b>2 min</b>	<b>1 min</b>
Mean Difference (95% CI)	1.81 (0.38 to 3.25)	0.78 (−0.93 to 2.50)	1.97 (−0.04 to 3.98)	3.19 (1.08 to 5.30)	4.88 (1.93 to 7.82)	6.50 (2.68 to 10.32)	
Upper LOA	9.61 (7.12 to 12.10)	10.09 (7.12 to 13.06)	12.88 (9.40 to 16.36)	14.65 (10.10 to 18.31)	20.85 (15.75 to 25.95)	27.22 (20.61 to 33.83)	
Lower LOA	−5.99 (−8.47 to −3.50)	−8.53 (−11.50 to −5.56)	−8.94 (−12.43 to −5.46)	−8.28 (−11.94 to −4.62)	−11.10 (−16.20 to −6.00)	−14.22 (−20.84 to −7.61)	
SD	3.98	4.75	5.57	5.85	8.15	10.57	
P* (F test)	0.607	0.643	0.182	0.109	0.0008	<0.00001	

CI, Confidence interval; LOA, limit of agreement; SD, standard deviation  
\* Using F test to compare the variances with intra-observer study on the 8-minute images datasets

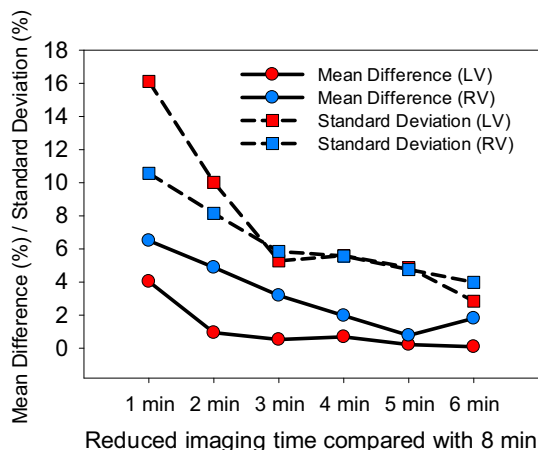


**Figure 6.** Bland-Altman analyses comparing the agreement between reduced imaging time and 8-minute acquisition time with CZT-SPECT.

and scatter images without additional radiation exposure to patients.<sup>24</sup> Further study is necessary to determine whether AC significantly affects EFs measured from the CZT camera.

GBPS is typically acquired in 8- or 16-frames owing to the lower count density of traditional NaI cameras, while planar ERNA is recorded using the 24-frame mode. The selected frame number per cycle may affect count statistics in the individual frame, and may introduce errors in EF measurements. Since the new CZT camera has improved count sensitivity, NaI-planar, CZT-SPECT, and CZT-repro datasets were compared using the 24-frame mode in our study to avoid bias. However, the CZT-SPECT dataset was reconstructed into 16-frame instead of 24-frame mode due to the software limitation when accessing reduced imaging acquisition time. Previous studies demonstrated LVEF and RVEF calculated with 8-frame GBPS using the NaI camera correlated well with that of 16-frame GBPS, showing no statistical differences in measurements.<sup>25,26</sup> Nonetheless, a higher number of frames used may confer poorer statistical quality to each image set; therefore a longer acquisition time may be required to achieve adequate image quality. Further studies are needed to validate whether the suggested 4-minute acquisition time in our study can also be applied using the 24-frame mode acquisition.

The major limitation of the study, as already mentioned above, is lack of standard reference. Currently, planar ERNA is still widely used as clinical routine, including Taiwan. Many studies have confirmed the good correlation of biventricular EF functions by planar ERNA, GBPS, and cardiac MRI.<sup>3,4,15</sup> Although high cost and time-consuming procedure of cardiac MRI makes it less available in clinical practice,<sup>4</sup> it is

considered as the gold standard for measurement of ventricular functions.<sup>15</sup> Further comparison studies, especially RV and LV in patients with LV systolic dysfunction should be warranted.

## NEW KNOWLEDGE GAINED

Biventricular EFs obtained from the re-projected planar images of CZT-SPECT correlated best with planar ERNA method from NaI detectors, overcoming the issue of overlapping cardiac chambers. The imaging time can be reduced as short as 4 minutes while preserving image quality. Correlations were better in patients with LVEF  $\geq 35\%$  than those with LVEF  $< 35\%$ . Moreover, inter- and intra-observer reliability were consistently satisfactory for LV volumes and EFs, while less satisfactory inter-observer variation of RV volumetric measurements.

## CONCLUSIONS

The new dedicated cardiac CZT-SPECT camera has the ability to replace the planar NaI detector when performing ERNA. CZT-SPECT and CZT-repro correlated well with NaI-planar in the assessment of left ventricular function. This study also suggests that imaging time can be reduced to as short as 4 minutes while preserving image quality in the assessment of biventricular EFs using the CZT camera.

## Acknowledgments

*This study was supported in part by Ministry of Science and Technology of Taiwan (MOST 101-2314-B-418-012-MY3 and 103-NU-E-002-001-NU). No other potential conflict of interest relevant to this article was reported.*

## Disclosures

*The authors have disclosed that they do not have any potential conflicts of interest.*

## References

- de Geus-Oei LF, Mavinkurve-Groothuis AM, Bellersen L, Gotthardt M, Oyen WJ, Kapusta L, et al. Scintigraphic techniques for early detection of cancer treatment-induced cardiotoxicity. *J Nucl Med Technol* 2013;41:170-81.
- Daou D, Van Krieking SD, Coaguila C, Lebtahi R, Fourme T, Sitbon O, et al. Automatic quantification of right ventricular function with gated blood pool SPECT. *J Nucl Cardiol* 2004;11:293-304.
- Groch MW, DePuey EG, Belzberg AC, Erwin WD, Kamran M, Barnett CA, et al. Planar imaging versus gated blood-pool SPECT for the assessment of ventricular performance: A multicenter study. *J Nucl Med* 2001;42:1773-9.

4. Sibille L, Bouallegue FB, Bourdon A, Micheau A, Vernhet-Kovacsik H, Mariano-Goulart D. Comparative values of gated blood-pool SPECT and CMR for ejection fraction and volume estimation. *Nucl Med Commun* 2011;32:121-8.
5. Herzog BA, Buechel RR, Katz R, Brueckner M, Husmann L, Burger IA, et al. Nuclear myocardial perfusion imaging with a cadmium-zinc-telluride detector technique: Optimized protocol for scan time reduction. *J Nucl Med* 2010;51:46-51.
6. Duvall WL, Croft LB, Ginsberg ES, Einstein AJ, Guma KA, George T, et al. Reduced isotope dose and imaging time with a high-efficiency CZT SPECT camera. *J Nucl Cardiol* 2011;18:847-57.
7. Einstein AJ, Blankstein R, Andrews H, Fish M, Padgett R, Hayes SW, et al. Comparison of image quality, myocardial perfusion, and left ventricular function between standard imaging and single-injection ultra-low-dose imaging using a high-efficiency SPECT camera: The MILLISIEVERT study. *J Nucl Med* 2014;55:1430-7.
8. Wells RG, Marvin B, Kovalski G, Ruddy TD. Planar radionuclide angiography with a dedicated cardiac SPECT camera. *J Nucl Cardiol* 2013;20:358-66.
9. Jensen MM, Schmidt U, Huang C, Zerahn B. Gated tomographic radionuclide angiography using cadmium-zinc-telluride detector gamma camera; comparison to traditional gamma cameras. *J Nucl Cardiol* 2014;21:384-96.
10. Jensen MM, Haase C, Zerahn B. Interstudy repeatability of left and right ventricular volume estimations by serial-gated tomographic radionuclide angiographies using a cadmium-zinc-telluride detector gamma camera. *Clin Physiol Funct Imaging* 2015;35:418-24.
11. Corbett JR, Akinboboye OO, Bacharach SL, Borer JS, Botvinick EH, DePuey EG, et al. Equilibrium radionuclide angiocardiology. *J Nucl Cardiol* 2006;13:e56-79.
12. Massardo T, Gal RA, Grenier RP, Schmidt DH, Port SC. Left ventricular volume calculation using a count-based ratio method applied to multigated radionuclide angiography. *J Nucl Med* 1990;31:450-6.
13. Van Kriekinge SD, Berman DS, Germano G. Automatic quantification of left ventricular ejection fraction from gated blood pool SPECT. *J Nucl Cardiol* 1999;6:498-506.
14. O'Doherty J, Rojas Fisher B, Price JM, Wechalekar K. Assessment of an intermediate reprojection technique transitioning from planar to SPECT radionuclide ventriculography. *J Nucl Cardiol* 2014;21:944-53.
15. Xie BQ, Tian YQ, Zhang J, Zhao SH, Yang MF, Guo F, et al. Evaluation of left and right ventricular ejection fraction and volumes from gated blood-pool SPECT in patients with dilated cardiomyopathy: Comparison with cardiac MRI. *J Nucl Med* 2012;53:584-91.
16. Massardo T, Jaimovich R, Lavados H, Gutierrez D, Rodriguez JC, Saavedra JM, et al. Comparison of radionuclide ventriculography using SPECT and planar techniques in different cardiac conditions. *Eur J Nucl Med Mol Imaging* 2007;34:1735-46.
17. Nichols K, Saouaf R, Ababneh AA, Barst RJ, Rosenbaum MS, Groch MW, et al. Validation of SPECT equilibrium radionuclide angiographic right ventricular parameters by cardiac magnetic resonance imaging. *J Nucl Cardiol* 2002;9:153-60.
18. Hacker M, Hoyer X, Kupzyk S, La Fougere C, Kois J, Stempfle HU, et al. Clinical validation of the gated blood pool SPECT QBS processing software in congestive heart failure patients: Correlation with MUGA, first-pass RNV and 2D-echocardiography. *Int J Cardiovasc Imaging* 2006;22:407-16.
19. Schwartz RG, McKenzie WB, Alexander J, Sager P, D'Souza A, Manatunga A, et al. Congestive heart failure and left ventricular dysfunction complicating doxorubicin therapy. Seven-year experience using serial radionuclide angiocardiology. *Am J Med* 1987;82:1109-18.
20. Songy B, Guernou M, Lussato D, Queneau M, Geronazzo R. Low-dose thallium-201 protocol with a cadmium-zinc-telluride cardiac camera. *Nucl Med Commun* 2012;33:464-9.
21. Oddstig J, Hedeer F, Jogi J, Carlsson M, Hindorf C, Engblom H. Reduced administered activity, reduced acquisition time, and preserved image quality for the new CZT camera. *J Nucl Cardiol* 2013;20:38-44.
22. Sibille L, Bouallegue FB, Bourdon A, Mariano-Goulart D. Influence of CT-based attenuation correction in assessment of left and right ventricular functions with count-based gated blood-pool SPECT. *J Nucl Cardiol* 2011;18:642-9.
23. Liu CJ, Cheng JS, Chen YC, Huang YH, Yen RF. A performance comparison of novel cadmium-zinc-telluride camera and conventional SPECT/CT using anthropomorphic torso phantom and water bags to simulate soft tissue and breast attenuation. *Ann Nucl Med* 2015;29:342-50.
24. Yamauchi Y, Kanzaki Y, Otsuka K, Hayashi M, Okada M, Nogi S, et al. Novel attenuation correction of SPECT images using scatter photopeak window data for the detection of coronary artery disease. *J Nucl Cardiol* 2014;21:109-17.
25. Kim SJ, Kim IJ, Kim YS, Kim YK. Gated blood pool SPECT for measurement of left ventricular volumes and left ventricular ejection fraction: Comparison of 8 and 16 frame gated blood pool SPECT. *Int J Cardiovasc Imaging* 2005;21:261-6.
26. Kim SJ, Kim IJ, Kim YS, Kim YK, Shin YB, Kim DS. Automatic quantification of right ventricular volumes and right ventricular ejection fraction with gated blood pool SPECT: Comparison of 8- and 16-frame gated blood pool SPECT with first-pass radionuclide angiography. *J Nucl Cardiol* 2005;12:553-9.